(34) Swan, P. R. *J. Polym. Sci.* **1962**, *56*, 403.
(35) Davis, G. T.; Eby, R. K.; Colson, J. P. *J. Appl. Phys.* **1970**, *41*, 4316.
(36) Swan, P. R. *J. Polym. Sci.* **1960**, *42*, 525.
(37) Wilkinson, D. A.; Nagle, J. F. *Biochim. Biophys. Acta* **1982**, *688*, 107.
(38) Kaplan, J. I.; Drauglis, E. *Chem. Phys. Lett.* **1971**, *9*, 645.
(39) Wulf, A. *J. Chem. Phys.* **1976**, *64*, 104.
(40) Zwanzig, R. *J. Chem. Phys.* **1963**, *39*, 2251.
(41) Richardson, M. J.; Flory, P. J.; Jackson, J. B. *Polymer* **1963**, *4*, 221.
(42) Bunn, C. W. *J. Polym. Sci.* **1955**, *16*, 323.
(43) Volkenstein, M. V. "Configurational Statistics of Polymer Chains"; (translated by Timasheff, S. N.; Timasheff, M. J.) Wiley-Interscience: New York, 1963.
(44) Gujrati, P. D.; Goldstein, M. *J. Phys. Chem.* **1980**, *84*, 859.
(45) Nagle, J. F. *J. Stat. Phys.* **1985**, *38*, 531.
(46) Gujrati, P. D. *J. Phys. A: Math. Gen.* **1980**, *13*, L437.
(47) Gujrati, P. D.; Goldstein, M. *J. Chem. Phys.* **1981**, *74*, 2596.
(48) Gujrati, P. D. *J. Stat. Phys.* **1982**, *28*, 441.
(49) Huggins, M. L. *Ann. N.Y. Acad. Sci.* **1942**, *43*, 1.
(50) Gibbs, J. H.; DiMarzio, E. A. *J. Chem. Phys.* **1958**, *28*, 373.
(51) Mandelkern, L. "Crystallization of Polymers"; McGraw-Hill: New York, 1964. See especially section 5-3, p 130 and section 5-4, pp 131-138.
(52) Slater, J. C. "Introduction to Chemical Physics"; McGraw-Hill: New York, 1939; p 260-262 and 220-221.
(53) Oriani, R. A. *J. Chem. Phys.* **1951**, *19*, 93.
(54) Temperley, H. N. V. *J. Res. Natl. Bur. Stand. U. S.* **1956**, *56*, 55.
(55) Tonelli, A. E. *Anal. Calorim.* **1974**, *3*, 89.
(56) Allen, G. *J. Appl. Chem.* **1964**, *14*, 1.
(57) Fortune, G. C.; Malcolm, G. N. *J. Phys. Chem.* **1967**, *71*, 876.
(58) Karasz, F. E.; Couchman, P. R.; Klempner, D. *Macromolecules* **1977**, *10*, 88.
(59) Kubaschewski, O. *Trans. Faraday Soc.* **1949**, *45*, 931.

Phenomenological Relationship between Dielectric Relaxation and Thermodynamic Recovery Processes near the Glass Transition

S. Matsuoka,* G. Williams,† G. E. Johnson, E. W. Anderson, and T. Furukawa‡

AT&T Bell Laboratories, Murray Hill, New Jersey 07974. *Received March 4, 1985*

ABSTRACT: Applying the experimental dielectric relaxation spectrum of amorphous poly(vinyl acetate) in the form of Dirac δ's over 6 decades of time to the basic nonlinear differential equation for the thermodynamic recovery process accurately reproduced volume relaxation data. Experimental dielectric relaxation time follows the Vogel-Fulcher (or WLF) equation, as is well-known. The thermodynamic recovery time from volume data[5] was found to be precisely equal to the dielectric relaxation time near T_g but at lower temperatures to diverge from the extrapolation of the dielectric data. The recovery time will depend on the fictive temperature following the *same* Vogel formula rather than Narayanaswamy's formula, but its temperature dependence follows the Arrhenius formula. The shift of the relaxation time with aging was calculated from the equations thus evaluated and was shown to agree with viscoelastic and dielectric data, clearly showing that this relaxation time should not be confused with the "effective" τ obtained from the overall rate of thermodynamic recovery. These phenomena are common to polymers and nonpolymers, since both poly(vinyl acetate) and glucose were found to exhibit all of the physical properties that are essential to the behavior studied.

The physics of slow relaxation processes in glass-forming liquids continue to interest many workers. Substantial progress has been made on the phenomenological understanding of the thermodynamic recovery process due notably to the work of Moynihan and co-workers,[1-3] and Kovacs and co-workers,[4,5] through the introduction of the distribution of relaxation times superimposed on the nonlinear dependence of relaxation time on the change of the structure. Their fundamental differential equations are essentially the same nonlinear equation with distributed order parameters. Moynihan (M model) invoked the Kohlrausch-Williams-Watts relaxation function,[6] while Kovacs, Aklonis, Hutchinson, and Ramos[4] (KAHR model) used a double box-shaped distribution of relaxation times. The variations in density fluctuations at various stages of recovery were implied in the solution of the differential equation, but the relaxation spectrum was assumed to remain unchanged throughout the recovery process. Both, as well as others who have studied similar problems extensively,[7-9] utilized the formula of Tool[10] or Narayanaswamy[11] for the temperature and structure dependence of the relaxation spectrum, which is reduced to an Arrhenius type dependence with an extremely large activation energy along the equilibrium liquidus line.

A bothersome question remains still unresolved with respect to the relationship between the dielectric or viscoelastic relaxation time and the volume or enthalpy relaxation (recovery) time extrapolated to equilibrium. Kovacs, Stratton, and Ferry[12] have shown that the viscoelastic and volumetric data near T_g do not coincide with the curve calculated from data obtained at higher temperatures. Sasabe and Moynihan[2] have also shown that the extrapolation of dielectric data from high temperature does not coincide with the enthalpic data near T_g. Yet the work presented here will show that the basic distribution of the recovery times can be assumed to be essentially the same as the relaxation spectrum and, moreover, that the relaxation and the recovery times do coincide near the glass temperature. Indeed, if there were no relationship at all between the two relaxation processes, it would be even more difficult to explain some of the empirical links that seem to exist between the two processes.

In this work we have applied the experimental dielectric spectrum as the order parameters to the essentially same basic differential equation used by all these workers. Our model has an advantage to allow for adding a number of possible variations. In the process we have learned that the Arrhenius type structure term in Narayanaswamy's equation should be replaced by the Vogel type formula.[13] Since in our study each order parameter can be traced during the aging (recovery) process, we were also able to

† Permanent address: The University College of Wales, Aberystwyth, Dyfed SY23 1NE, United Kingdom.
‡ Permanent address: The Institute of Physics and Chemical Research, 2-1, Hirosawa, Wako-shi, Saitama 351, Japan.

0024-9297/85/2218-2652$01.50/0

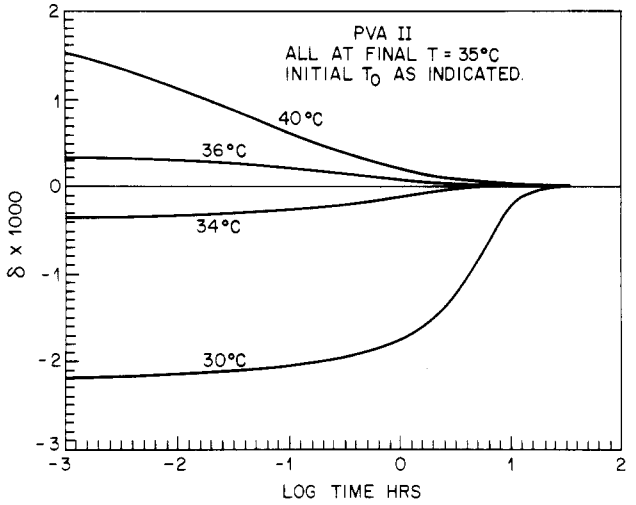

Figure 1. Calculated curves for isothermal volume change from the initial temperatures as indicated to the final temperature of 35 °C, using eq 14 with $[\log \tau]_{T_1} = -0.6$ (h), $T_1 = 309$ K, $T_2 = 257.5$ K, $H_a = 56$ kcal mol^{-1}, $H_w = 3.70$ kcal mol^{-1}, and $\Delta\alpha = 3.71 \times 10^{-4}$ °C^{-1}.

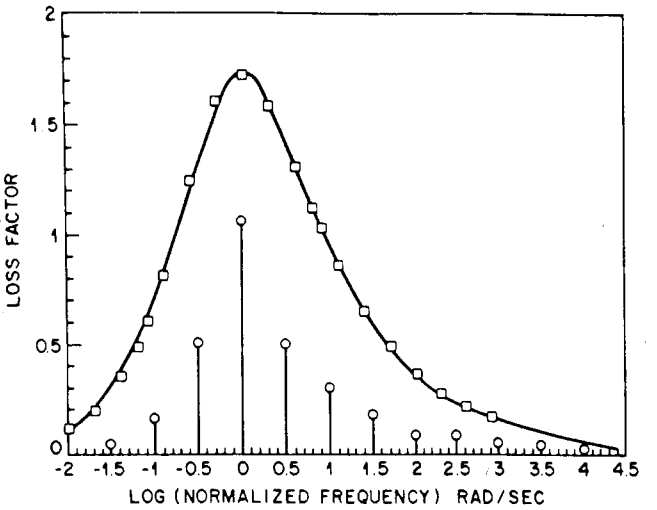

Figure 2. Dielectric loss factor (□) for poly(vinyl acetate) at 50 °C normalized along the logarithmic frequency scale is reproduced by the sum of the Dirac δ (○) $x[\omega\tau/(1+\omega^2\tau^2)]$. Solid line is that calculated from the sum of the individual processes indicated in the figure.

show that the characteristic relaxation time should not be confused with τ_{eff} with respect to their dependence on the temperature, structure, and history.

Differential Equation for the Relaxation Process

The relaxation process may be described as a time-dependent process for a system to return from a perturbed state to the equilibrium state. The differential equation for the rate of relaxation at a constant temperature is

$$-d\delta/dt = \delta/\tau \tag{1}$$

where δ is the deviation from equilibrium of the stress, enthalpy, volume, etc. For example, $\delta = (v - v_\infty)/v_\infty$, where v is the specific volume in the nonequilibrium state and v_∞ is that in the equilibrium state. In the simplest case where the deviation is small enough to have a negligible effect on the magnitude of the relaxation time, τ, as in dielectric relaxation, and where, moreover, the relaxation process is controlled by a single rate constant, $1/\tau$, such as with dipole orientation in some hydrogen-bonded liquids, the above differential equation is *linear* and the solution of this one-parameter differential equation in response to a step type perturbation is simply

$$\delta(t) = \delta_0 \exp(-t/\tau) \tag{2}$$

The assumption of the linearity is valid only in the case with very small perturbation. It is generally expected that the deviation, δ, will affect the relaxation time, and the differential equation will therefore be nonlinear. Similarly, the assumption of the single relaxation time is not valid with most liquids near T_g.

In Figure 1, four calculated volume recovery curves are shown for poly(vinyl acetate) following a sudden change in temperature from various initial temperatures to the final temperature of 35 °C. The calculation is based on the procedure to be described subsequently. The purpose of showing these curves, which are in agreement with the experimental data,[4] is to show a distinction between linear and nonlinear responses, which depend on both the magnitude and the sign of the temperature jump. For the jump of ±1 °C, the response curves are almost symmetrical against the abscissa, and this feature denotes the validity of assuming the linear differential equation. Their flat shape is almost totally the reflection of the distribution of the relaxation times.

When the relaxation process is controlled by a multiple number of rate constants, $1/\tau_i$ but the deviation, δ, is still small enough that it does not significantly affect the magnitude of each relaxation time, i.e., *linear*, the overall rate of relaxation can be considered as the sum of the individual relaxation processes superimposed on each other with the weighting factor G_i for each τ_i such that

$$-\frac{d\delta}{dt} = -\sum_i G_i \frac{d\delta_i}{dt} = \sum_i G_i \delta_i/\tau_i \tag{3}$$

where G_i is normalized to result in $\sum G_i = 1$. The quantity δ_i can be defined as $\delta_i = (v_i - v_{i\infty})/v_{i\infty}$, where v_i is the specific volume of the ith element and $v_{i\infty}$ is its equilibrium value. There is no reason to assume that all $v_{i\infty}$'s must be equal. In fact, since each element is assumed to exhibit a different relaxation time, τ_i, each $v_{i\infty}$ may be considered to be different from $v_{j\infty}$ in general. Thus in this work $\delta = \sum G_i\delta_i$ and not $\delta = \sum \delta_i$ as defined by other workers.[4,7]

In Figure 2, the dielectric loss factor for poly(vinyl acetate) is shown vs. the logarithmic frequency scaled so that its peak coincides with the frequency of 1 rad/s. A set of 12 Dirac δ's with proper weighting factor G_i's were evaluated so that the sum according to the equation shown below will precisely reproduce the loss factor, ϵ'', vs. frequency data

$$\epsilon''(\omega) = \sum_i G_i \omega\tau_i/(1+\omega^2\tau_i^2) \tag{4}$$

Moynihan et al. (M model) did not use the differential equation such as eq 3 directly. Instead, they worked with the solutions of the differential equation in response to specific temperature histories. The solution of the *linear* differential equation for $\delta(t)$ in response to the step type perturbation, according to the M model, is made to conform to the Kohlrausch–Williams–Watts formula[6]

$$\delta(t) = G_0 \exp\{-(t/\tau_0)^\beta\} \tag{5a}$$

where τ_0 is the characteristic relaxation time and β is an empirical parameter whose value is usually about 0.5. These authors assumed that the distribution of relaxation times should remain unchanged; therefore β is constant, and τ_0 and all types of "mean" relaxation time, τ_{av}, will maintain a simple relationship, τ_0/τ_{av} = constant.

With models that deal directly with a fixed relaxation spectrum, such as the KAHR model and our model, the characteristic relaxation time can be taken to mean any

relaxation time whose magnitude with respect to the rest of the spectrum is fixed. In our model we have chosen the relaxation time, τ_{max}, that corresponds to the dielectric loss maximum as the characteristic relaxation time. This characteristic relaxation time is proportional to the mean τ_{av}, defined as $\ln \tau_{av} = \sum G_i \ln \tau_i$, and the shift of the entire spectrum of relaxation times can be specified by the shift in either τ_{max} or τ_{av}. The shape of the distribution of relaxation times shown in Figure 2 is common to many polymeric and nonpolymeric materials near the primary glass transition, and it is well-known[6] that the relaxation function, $\phi(t)$, can be approximated by the formula

$$\phi(t) = \sum G_i \exp(-t/\tau_i) = G_0 \exp\{-(t/\tau)^\beta\} \quad (5b)$$

Our data can be shown to fit well with $\beta = 0.42$, with log τ_0 in eq 5a equal to log τ_{max} + 0.5.

For the jump of ±5 °C, the response curves in Figure 1 are seen as highly asymmetrical against the abscissa, clearly indicating the dependence of τ on δ such that the linearity cannot be assumed. The nonlinearity is the manifestation of the difference in the initial relaxation time when starting from above as compared to from below the final temperature. Thus the structural dependence of the rate of relaxation must be included in the formulation. The M model again does not directly evaluate the differential equation but incorporates the relaxation function, $\phi(t)$ (which is essentially $\delta(t)$ in response to the step-type perturbation) of the form

$$\phi(t) = \exp\left[-\left(\int_0^t dt'/\tau_0(t')\right)^\beta\right] \quad (5c)$$

and $\tau_0(t)$ in turn to depend on the temperature and the structural parameter called the fictive temperature in the manner to be discussed in the following section. With the KAHR model as well as our model, the entire spectrum of relaxation times is shifted without change in its shape in accordance with the change in the temperature and the fictive temperature.

It is sometimes convenient to invoke a structural parameter known as the fictive temperature, T_f, which is an extensive thermodynamic quantity in spite of its name. It is defined as the temperature at which the volume/enthalpy/entropy of a glass having had a particular thermodynamic history and therefore presumably possessing a unique structure (though this point will be shown to be questionable) intersects the equilibrium liquidus line. Thus the fictive temperature is related to δ by the formula

$$\delta = \Delta\alpha(T_f - T) \quad (6)$$

where $\Delta\alpha$ is the difference in thermal expansion coefficients, the specific heats, or the specific heats divided by the temperature between the liquid and the glass if δ is for the volume, enthalpy, or entropy, respectively.

One conclusive piece of evidence that a single relaxation time model is bound to fail is Kovacs's data on the so-called memory effect.[5] As shown in the schematic volume–temperature curve in Figure 3, the experiment is started in equilibrium at point G at a high temperature, followed by a sudden change to point A; thereupon the volume begins to decrease. Point B is reached after waiting for a proper period of time; the temperature is now suddenly increased to point E, which has been, by design, calculated to be precisely on the equilibrium liquidus line. Kovacs' data showed, as well-known to the workers in this field, that the volume first increases away from the equilibrium point E toward point F, and after going through a maximum, drifts back toward the original equilibrium point E. The last part of this excursion in volume vs. time always coincides with the volume relaxation upon simple quenching from G to F followed by relaxation to E. The magnitude of the excursion was found to increase for the greater initial temperature difference from G to A. Both models that have been cited above are similar in assuming that the distribution of relaxation times is responsible for this effect, namely, that the components with longer relaxation times will undergo the volume change more slowly and the components with shorter relaxation times will undergo the volume change more quickly. Summing up all of these components will obtain the total volume, meaning that the same volume and the same average fictive temperature do not necessarily mean the identical state. In their movement from point A to B, the faster-moving components have passed B, while the slower components have not reached there yet. Bringing this state suddenly to E will result in the fast-moving components below the point B rising while the slow-moving components continue their densification. The volume change in the early stage after E is reached is dominated by the increase of the fast components, but after a while the fast-moving components will have reached the equilibrium value at E one by one while the slower-moving components still continue their descent toward E, and thus the overall volume after reaching the maximum will follow the isothermal contraction curve that followed a simple quench from T_0 to T. Moynihan[1] is the first to formulate such a model, utilizing the Kohlrausch–Williams–Watts type continuous distribution function for the relaxation times such that at the time when the temperature was changed from B to E the integral is split into the portion that continues to decrease (the longer relaxation times) and the portion that reverses direction toward the new equilibrium value at the new temperature.

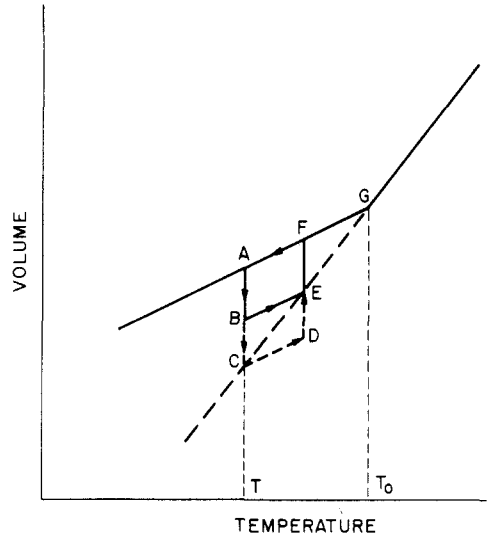

Figure 3. Schematic diagram for the volume vs. temperature near glass transition.

With our model, δ is divided into components δ_i, such that $\delta = \sum G_i \delta_i$, and the rate of relaxation for each δ_i is assumed to be controlled by the corresponding relaxation time, τ_i

$$-d\delta_i/dt = \delta_i/\tau_i \quad (7)$$

and τ_i is calculated from the characteristic relaxation time, τ_0, by assuming that the distribution of relaxation times remains the same at all times

$$\tau_i = a_i \tau_0 \quad (8)$$

where a_i is a constant independent of T, T_f, t, τ_0, etc., and τ_0 can be set equal to average τ_{av}. Since τ_0 and τ_{av} are interchangeably used, we simply designated both as τ here.

Equation 8 suggests that the change in δ_i with time is coupled to the overall δ. We have actually examined and found that if individual δ_i are assumed to shift independently with their own τ_i uncoupled, the calculated recovery results would not agree with Kovacs' data.[4] τ is uniquely determined by the overall deviation, δ

$$\tau = f(T,\delta,\tau_{0e}) \tag{9}$$

where τ_{0e} is τ in the equilibrium state at a reference temperature; the function $f(T,\delta,\tau_{0e})$ suggests the existence of a unique relationship between τ and the fictive temperature, T_f, since δ is uniquely related to T_f as will be shown below. Thus the shift in relaxation times with aging can be specified by one order parameter, even though the values of δ_i are changing further and further apart from each other during aging. $1/\tau$ is *not* equal to $(-d\delta/dt)/\delta$, though $1/\tau$ is clearly proportional to $\sum(1/\tau_i)$ in order to be consistent with eq 8 and the rate of change for δ_i, or $(-d\delta_i/dt)/\delta_i$, *is* always equal to $1/\tau_i$ by eq 7. In turn, each τ_i is *not* equal to $f(T,\delta_i,\tau_{0e})$ unlike the relationship that exists for τ with δ in eq 9. Each τ_i is calculated from τ according to eq 8, and τ is obtained from δ and δ from the weighted sum of δ_i.

A simple example with a quenching experiment may be used to further clarify the physical significance of the calculation steps. Initially at equilibrium at T_0, $\delta = 0$ and all δ_i are also zero. After a sudden cooling, the slow- and the fast-recovering components initially assume the same value for the deviation from the equilibrium; i.e., $\delta_i = \delta_j = \delta$. With the passing of time, however, the slow component, e.g., δ_1, with a long relaxation time, τ_1 (which is also changing with time), decreases much more slowly than the fast-recovering component, e.g., δ_9, with the short relaxation time, τ_9. Thus the difference between δ_1 and δ_9 continues to widen until δ_9 reaches 0 at the new equilibrium. Meanwhile, the ratio of τ_1 to τ_9 is maintained as constant. Thus the slow and fast density fluctuations become more widely separated in the nonequilibrium state, while the spread of correlation times is kept constant, the density of the *slower* component remains *low*, and the density of the *faster* component rapidly becomes *higher*. Moynihan's model, which assumes the parameter β to be constant, is equivalent to assuming a constant spread of discrete ln τ_i such as with the KAHR model.

Computational Procedure

A very short and simple program suitable for a personal computer has been constructed. The steps are shown as follows:

10 Enter the data of the distribution of relaxation times, $G(j)$ and $\tau(j)$, of Figure 2. ($G(j)$ values need not be normalized to meet $\sum G(j) = 1$.)

20 Initial temperature T_0 is changed to the new temperature T, whereupon the time begins to increase by the increment of $\Delta \log t$.

30 Initial fictive temperature T_f is set equal to T_0, and δ is calculated from eq 6.

40 Initial individual $\delta(j)$'s are all same, being equal to δ.

50 Calculate log τ_{max}, which depends on T and T_f according to the function that will be discussed in the following section.

60 Calculate log $\tau(j)$ for each individual Dirac δ ($G(j)$, $\tau(j)$) by the same spread in $\tau(j)/\tau$ as in the original distribution; cf. eq 8.

70 Calculate each new $\delta(j)$ by changing it by the increment obtained from the difference equation, equivalent to the nonlinear version of the differential equation, eq 6, or

$$\Delta\delta(j) = (-\delta(j))\{1 - \exp(\Delta t/\tau(j))\} \tag{10}$$

80 Calculate new $\delta = \sum G(j)\delta(j)/\sum G(j)$ and new T_f from eq 6.

90 δ is plotted vs. log t; $\Delta\log t$ is added to log t and now go back to 50 and repeat. The above program also can be applied to the constant rate of change in temperature, instead of the constant temperature, to calculate the differential scanning calorimetry-type plot. In this case the increment $\Delta\log t$ is replaced by ΔT, and Δt in eq 10 by ΔT/heating or cooling rate.

In case of the memory effect, the computation is begun initially by quenching from T_0 at G to T at A in Figure 3. When T_f reaches T at E, the computation is halted, individual $T_f(j)$'s are printed out, and the new computation begins with those nonuniform $T_f(j)$'s as the initial values at the new temperature at E.

Before we decided on the above program as our final choice, many alternative models were tried. Among the models that were tried but failed to fit the data was a model in which each new $\tau(j)$ was calculated from the current values of T and $\delta(j)$ by using the master equation for $\tau(T,T_f)$ to be presented in the next section; i.e., the distribution of relaxation times is allowed to change. This trial model is equivalent to assuming that there is no coupling among the fluctuations, $\delta(j)$. This is found to be computationally unrealistic because the fast element, $\delta(j)$, must pass the adjacent slower element, $\delta(j-1)$, as time passes, and the portion of the spectrum with the initially shortest relaxation time can end up having the longest relaxation time. Another model was tried that assumed that there would be a distribution of fictive temperatures $T_f(j)$ at equilibrium according to the same master equation for $\tau(T,T_f)$. This works well provided that all $\tau(j)$'s at the new temperature are forced to conform to the same distribution; this implies that the same distribution of relaxation times is reestablished at each increment of time much faster than the time required for the shift of the overall average relaxation time, τ, to take place.

In summary, it was found that the distribution of relaxation times can be kept constant but the distribution of density fluctuations will change. The correlation between each component of the density fluctuation $\delta(j)$ and its corresponding relaxation time $\tau(j)$ therefore does not follow the functional relationship that exists between the overall density and the overall relaxation time, τ.

Temperature and Structural Dependence of the Relaxation Time

Sasabe and Moynihan[2] as well as Kovacs, Stratton, and Ferry[12] have shown that the apparent activation energy for the volumetric relaxation process near T_g is significantly greater than the apparent activation energy estimated from dielectric or viscoelastic relaxation data obtained at higher temperatures by, e.g., the Vogel–Fulcher formula.[13] Though it is difficult to identify a single "average" relaxation time for the distributed spectrum and the difficulty is compounded because of the limited range of temperature where the volume relaxation data can be obtained accurately and meaningfully, the magnitudes of these apparent activation energies are significantly different beyond the experimental or other margins of error.

The temperature dependence of the relaxation time in the equilibrium state may be interpreted in terms of a thermally activated process, but it may also be interpreted as arising indirectly through the change in structure that depends on the temperature. From the data taken only at equilibrium, there is no way of knowing how much or what fraction of it can be attributed to the former and the rest to the latter, even if such a simple division can be justified. Tool's[10] or Narayanaswamy's[11] equation exactly represents such a scheme, for example by dividing the Arrhenius equation into the temperature- and structure-

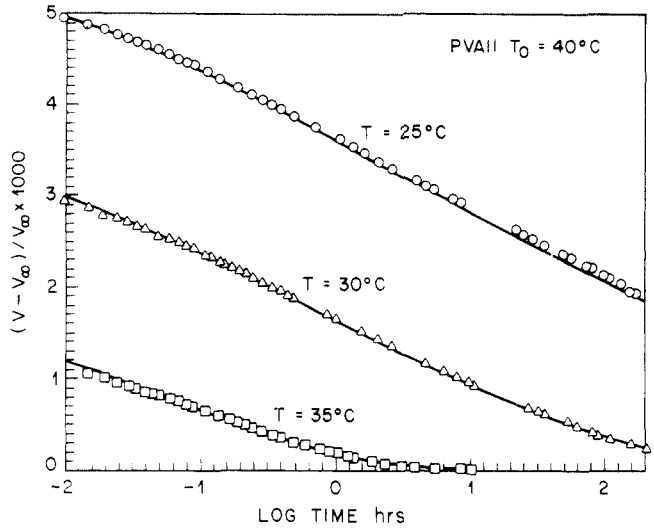

Figure 4. Isothermal contraction data of Kovacs, ref 5, reproduced by eq 14, using the same parameters cited in Figure 1.

dependent parts, the latter expressed in terms of the fictive temperature, T_f

$$\ln \tau = C + x\frac{H}{RT} + (1 - x)\frac{H}{RT_f} \tag{11}$$

where x is an adjustable parameter. At equilibrium on the liquidus line, $T_f = T$ and the equation is reduced to the simple Arrhenius relationship. Although this equation has been used by many authors,[1,4,7,8] we find that a better fit to Kovacs's volume recovery data is obtained if $(1 - x)H$ in eq 11 is allowed to increase with decreasing T_f, which is the characteristic of the Vogel–Fulcher formula. Replacement of the third term in eq 11 by the Vogel–Fulcher expression yields

$$\ln \tau = C + C'(T) + \frac{H_w}{R(T_f - T_2)} \tag{12}$$

which is used to fit the recovery data, where $C'(T)$ is an adjustable parameter for the temperature to be discussed subsequently. The values of 3.70 kcal mol^{-1} for H_w and 257.5 K for T_2 gave the best fit for one of the poly(vinyl acetate) samples studied by Kovacs,[5] as shown in Figure 4. Significantly, the equilibrium value for τ at $T_f = T =$ 35 °C lies exactly on the curve plotted for dielectric τ_{max} as shown in Figure 5a. The dielectric data shown were obtained on a special poly(vinyl acetate) sample that had been heated to 150 °C in vacuo. Also significantly, the values of the Vogel–Fulcher parameters, H_w and T_2, for T_f *only*, turned out to be equal to those for the dielectric relaxation time for the loss maximum, as shown by the open square points in Figure 5a. Thus the relaxation time for recovery curves extrapolated to the equilibrium, $T_f = T$, would have given a perfect fit to the dielectric relaxation time for the loss maximum if $C'(T)$ in eq 12 were independent of temperature. However, $C'(T)$ does depend on temperature; i.e., the recovery curves such as in Figure 4 must be shifted along the log t axis with different temperatures. The best fit for the temperature shift is obtained when $C'(T)$ is of the Arrhenius type, H_a/RT, with $H_a = 56$ kcal mol^{-1}. Thus the final formula for the recovery time is given by the equation

$$\ln \tau = C + \frac{H_a}{RT} + \frac{H_w}{R(T_f - T_2)} \tag{13}$$

which has the form of the equation proposed by Macedo and Litovitz.[30] The parameters for this formula were now evaluated from the data on the extensively analyzed

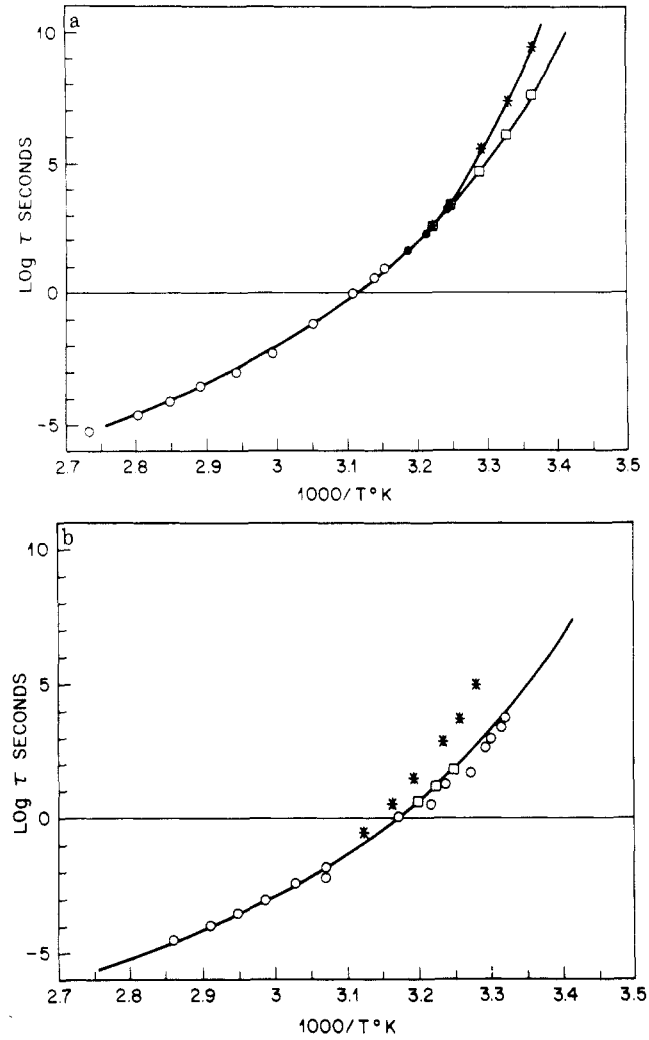

Figure 5. Logarithmic relaxation time vs. $1/T$ (K) for poly(vinyl acetate), PVA-II of ref 5 samples: (○) our dielectric log τ_{max}; (●) log τ_{max} obtained by shift of spectrometer data; (*) log τ_e obtained from volume data of Kovacs (ref 5) using eq 14; (□) log τ_e from eq 15, which includes only T_f dependence. Logarithmic relaxation time vs. $1/T$ (K) for poly(vinyl acetate), Moynihan et al. (ref 2): (○) dielectric data (ref 18); (*) log τ_e from enthalpic data (ref 2); (□) log τ_e from T_f dependence only (ref 2).

poly(vinyl acetate), PVA-II, by Kovacs,[5] and the following values were obtained for the equation

$$\ln \tau = [\ln \tau]_{T_1} + H_R/R(1/T - 1/T_1) + H_w/R\{1/(T_f - T_2) - 1/(T_1 - T_2)\} \tag{14}$$

where $T_1 = 309$ K, and $[\log \tau]_{T_1} = -0.6$ in units of hours. The differential equation for the rate of densification was evaluated with the computer program described earlier, using the value $\Delta\alpha = 3.71 \times 10^{-4}$ K^{-1}.

The equilibrium values obtained by setting $T_f = T$ in the above formula are plotted by the [*] in Figure 5a. The line is a plot obtained from the Vogel–Fulcher term only, by letting $T_f = T$

$$\ln \tau_f = [\ln \tau]_{T_1} + H_w/R\{1/(T - T_2) - 1/(T_1 - T_2)\} \tag{15}$$

This curve traces our own experimental dielectric data represented by open circles that were obtained on a poly(vinyl acetate) sample that was vigorously vacuum-dried at 150 °C and slowly cooled, resulting in about 2% total weight loss. Thus the T_f term of the recovery time lies exactly on the dielectric relaxation curve. A similar plot was made for comparing the enthalpic data obtained by Sasabe and Moynihan,[2] and the dielectric data by Mashimo et al.,[18] shown as [*] and [○], respectively. When

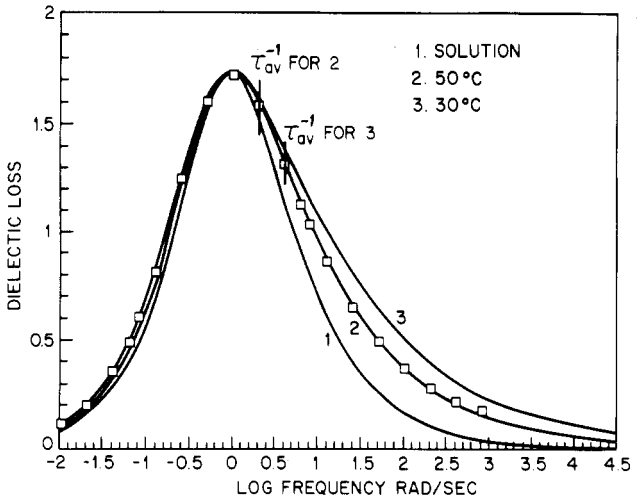

Figure 6. Spread of relaxation spectrum, which increases at lower temperature, ref 18.

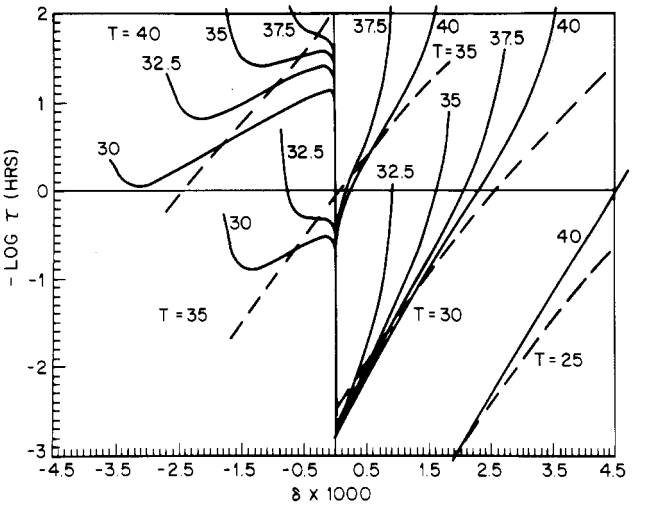

Figure 7. The rate constant log (d ln δ/dt) (—) and the relaxation time −log τ_{max} (---) vs. $\delta = (v - v_\infty)/v_\infty$ were calculated; the former is in good agreement with Kovacs' data[5] and the latter will be shown to agree with our dielectric and viscoelastic data. τ_{eff} is not the same as τ_{max}.

T_1 = 50 °C is chosen, the Vogel–Fulcher term in eq 9 indicated by the solid curve again matches their dielectric data exactly. Their data for the fictive temperature, when the inverse of the cooling rate is taken to be equal to the average relaxation time, fits well with this term also, as shown by [□].

The idea of two different formulas below and above the seemingly arbitrary temperature of T_1 is not pleasing, yet both Moynihan[2] and Kovacs et al.[12] had come to a similar conclusion. Before dismissing the Vogel–Fulcher equation simply as an empirical expression that failed near T_2, we should recall that the values of τ_e were evaluated from the kinetic data by extrapolating to the equilibrium condition, $T_f = T$ and that the extrapolation was carried out assuming a constant distribution of relaxation times. If the distribution of relaxation times should change systematically with the temperature, then the characteristic relaxation time calculated on the basis of a given distribution may have to be corrected at different temperatures. The viscoelastic relaxation spectrum below T_g has been found by Matsuoka et al.[34] (1) to shift during isothermal aging without changing the shape of the distribution, but (2) to change to progressively broader distributions at lower temperatures exhibiting smaller and smaller values of β for the Kohlrausch–Williams–Watts (KWW) parameter.[6] Item 1 is true only if all relaxing elements are aging at different rates but the distribution for such rates remains constant; this phenomenon is consistent with the model. The broader distribution at the lower temperature in item 2, on the other hand, is a reflection of the broader spread in δ_i during recovery, but the temperature-dependent breadth of the relaxation spectrum is not incorporated in the model, and the Arrhenius term in eq 13 may very well be needed to compensate for this.

In his model for the kinetics of structural relaxation, Brawer[16] has suggested that there is a rate-controlling fluctuation whose energy and structure determines the apparent free energy of activation. Another theory, recently proposed by Fredrickson and Andersen,[17] is based on the kinetics of an Ising model with restricted spin flips. These two theories tie together the increase of the apparent activation energy and the broadened relaxation times to the higher degree of cooperativity of structural relaxation at lower temperatures. In agreement with these two theories, the relaxation spectrum of poly(vinyl acetate) along the liquidus line in Figure 5b is broader at lower temperatures, as can be observed in Figure 6, whereas the broadening was barely observable for our sample.

The fact that the fictive temperature term in eq 13 matches exactly the equilibrium dielectric curve is in support of a generalized Adams–Gibbs[19] and Gibbs–DiMarzio[19] type model for the glass transition (which should not be restricted to polymers). Theories invoking free volume, such as one by Robertson, Simha, and Curro,[20] as well as Doolittle[21] and Turnbull and Cohen,[22] all lead also to the *fictive* temperature dependence, $H/R(T_f - T_2)$. Phillips has pointed out[29] that the Vogel–Fulcher type dependence really reflects the entropy as the criterion.

Another important feature of eq 13 is the functional relationship between the relaxation time and T_f and therefore δ. An arbitrary form for the δ dependence of τ, such as

$$\ln \tau = C + \gamma\delta \tag{16}$$

where γ is an empirical constant[23] and should be considered as an approximation when δ is kept small. A more general and appropriate formula would be a free volume formula such as a special Vogel–Fulcher formula in T_f

$$\ln \tau = C + H/R[\delta/\Delta\alpha + (T - T_2)] \tag{17}$$

where the quantity $[\delta/\Delta\alpha + (T - T_2)]$ is really a temperature-independent quantity, since it is equal to $T_f - T_2$.

Shift of Relaxation Spectrum during Aging

It is particularly desirable from an application viewpoint to know how the relaxation spectrum is shifted during thermodynamic aging. The solid curves in Figure 7 are the plots for the calculated (−log τ_{eff}), or the logarithmic rate of the volume change, log (−d ln δ/dt), vs. δ, which agrees well with Kovacs's data.[5] This quantity is *not* (−log τ_{max}), but it is nearly equal to the sum of all the rate constants for the individual δ_is. The true τ_{max} is the relaxation time corresponding to the Dirac δ at the loss maximum, or (G_4, τ_4) in this case, as shown in Figure 2. −log τ, or −log τ_{max}, is plotted with dotted lines in Figure 7 for comparison. The shift of relaxation spectrum must follow τ_{max} and not τ_{eff}. Since τ is a unique function of the temperature and δ (or T_f), τ from the positive side of δ meets with τ from the negative side of δ at the center where $\delta = 0$. The plot of −log τ vs. δ follows the one-parameter equation, which can be obtained by combining eq 13 and 17. Since the distribution of relaxation times is assumed to be unchanged at all times in the calculation, each in-

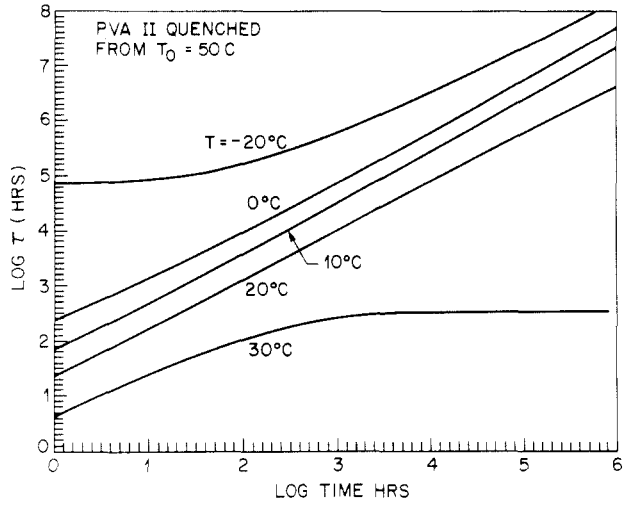

Figure 8. log τ_{max} vs. elapsed annealing (aging) time, following the quench from 50 °C to the temperature as indicated. Calculated for poly(vinyl acetate), PVA-II (ref 5).

dividual Dirac δ, (G_j, τ_j), also shifts in parallel with the main τ. The continuous shift of τ (and τ_j) slows down when the fast-moving δ_is reach equilibrium, but until then τ (and the rest of τ_js) is thus a fairly well-behaved function of time, as shown in Figure 8. The lines for T = 0, 10, and 20 °C are nearly straight, with the slope of d(ln τ)/d(ln t) ≈0.9. This slope can be shown to be ≈1 for a one-parameter model. At constant temperature, from eq 13 we can derive

$$\tau = \tau_0 \exp(1/(\delta + \epsilon)) \tag{18}$$

where $\epsilon = \Delta\alpha(T - T_2)$ is a constant at a given temperature T. This is equivalent to the WLF equation. Since $d\delta/dt = -\delta/\tau$ for the one-parameter model, differentiating τ with respect to t will obtain

$$d\tau/dt = \delta/(\delta + \epsilon)^2 \tag{19}$$

If we now assume $\tau/t = \delta/(\delta + \epsilon)^2$, then, the above condition will be met because it can be shown that

$$d\tau/dt = \tau/t(1 + 2(\delta + \epsilon)) - 1 \approx \delta/(\delta + \epsilon)^2$$

when $\delta \ll 1$ and $\delta + \epsilon \ll 1$. Thus we obtain that

$$d \ln \tau/d \ln t \approx 1 \tag{20}$$

namely the slope of nearly unity is predicted for the plot of log τ vs. log t if a one-parameter model can be used, except when near the equilibrium or initially if τ is too large as compared with t. If the distribution of the relaxation times is taken in consideration, the slope would be less than unity. As the equilibrium is approached, τ stops increasing so the slope, d ln τ/d ln t, will decrease, as shown by the curve for T = 30 °C in Figure 8. At very low temperatures, depending on the thermal history, the initial relaxation time can be too great for δ to be able to change significantly for some time. After time of the order of $\tau/100$, $(1/\delta \approx 40)$, δ begins to change significantly. If it was quenched from the higher temperature, the initial relaxation time would have been shorter and the increase in τ would have begun earlier.

Perhaps more germaine to the practical application is the case of heating an initially quenched glass to an elevated temperature that is still below T_g. This is the commonly practiced annealing process. The time dependence of the growing relaxation time for such a case is shown in Figure 9. Here PVA-II was first quenched from 50 to 10 °C, kept for the specified time, and then suddenly brought to the final temperature as specified. The momentary dip

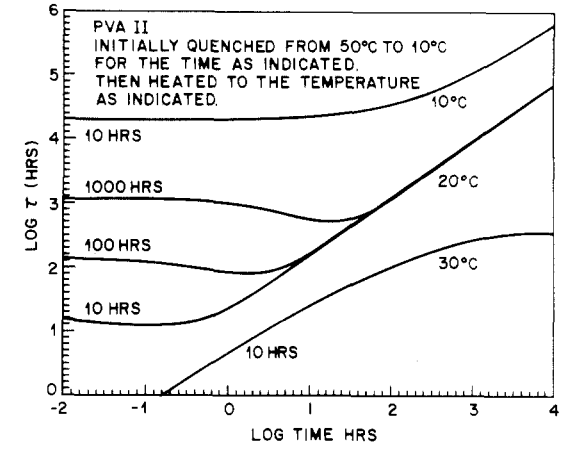

Figure 9. Relaxation time log τ_{max} vs. elapsed time following the history: 50 to 10 °C, held for the time indicated, and then heated to the temperature as indicated.

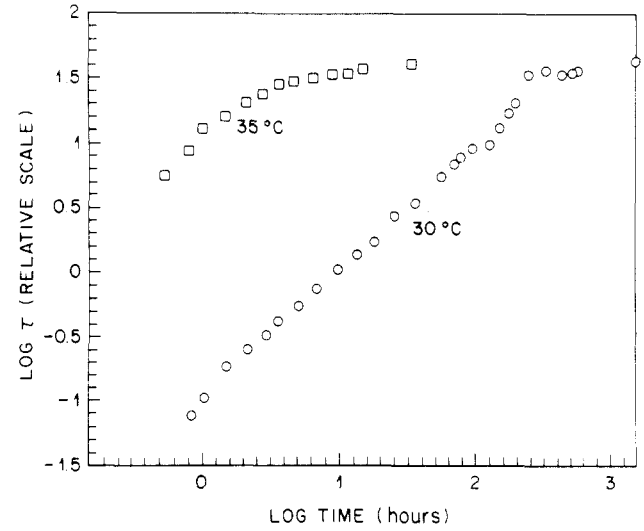

Figure 10. The logarithmic dielectric relaxation time (normalized as shift factor) increases linearly with the logarithmic time of annealing. Poly(vinyl acetate), PVA-II.

in the curves for T = 20 °C is a reflection of the high initial value of T_f in the quenched sample. These curves were calculated for τ, at loss maximum, or τ_4, but each Dirac δ (G_j, τ_j) also moves in parallel with the τ curves shown. Thus, by observing the high-frequency end of the spectrum, it is possible to estimate the movement of the entire spectrum. The central relaxation time in the glassy state is much too long to be observed by the dielectric measurement, since it is in the order of hours to 100 years as shown. However, since the shorter time end of the spectrum is about 3 decades removed from τ, it is possible to observe the change of τ_i with the Fourier transform dielectric spectrometer by recording the shift of the charge decay curve with the elapsed time. The experimental shift factor thus obtained at 30 and 35 °C are shown in Figure 10. The curve obtained at 30 °C is a straight line with a slope of nearly unity. It reaches the equilibrium at log t of about 2.5 (300 h). The curves labeled 30 °C in both Figures 8 and 9 reach the equilibrium at about log t of 2.5 also. Another interesting result found in Figure 7 is that the dotted line for log τ at T = 30 °C reaches δ = 0 (equilibrium) at the value of log τ = 2.5 (h). In the same Figure 7, it is noted that the dotted line for T = 35 °C intersects δ = 0 at log τ = 0. Going back to the experimental data of Figure 10, we note that the data taken at 35 °C reaches equilibrium also at about log t = 0. Going back to Figure 9, we see that for the average relaxation

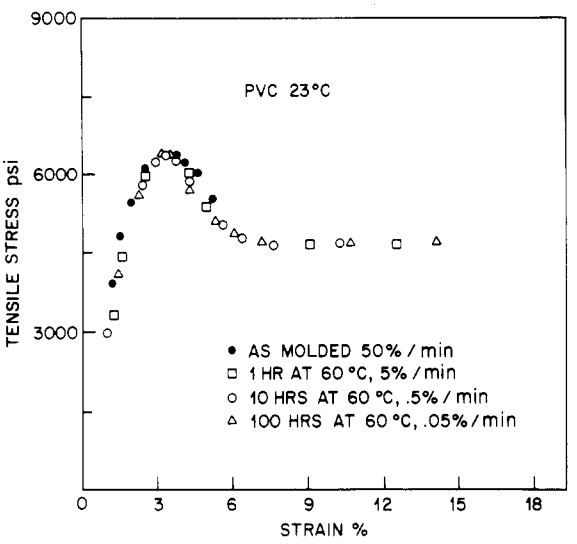

Figure 11. Stress–strain curves of four rigid poly(vinyl chloride) samples having undergone different thermal histories were strained at strain rates proportional to the time of annealing.

time to increase the value from 160 to 250 h at 30 °C, it takes about a year, meaning that the density fluctuations with the longer relaxation times would almost never come to the equilibrium state at this temperature. At 20 °C, the relaxation time continues to increase after 10^4 h or 1.14 years, with no signs of even nearing the equilibrium value.

The simple rule introduced here on the relationship between the shift of the relaxation spectrum and the time of annealing at an elevated temperature but below T_g should prove useful in predicting the effect of annealing on viscoelastic behavior of glassy polymers. Four stress strain curves at 23 °C for glassy poly(vinyl chloride) are shown in Figure 11, where among three of the four curves the product of the time spent on aging at 60 °C and the rate of strain are deliberately chosen to be the same. They all superimpose on each other. The fourth curve is for the as-molded sample, and its equivalent thermal history ought to be 0.1 h at 60 °C, since at the rate 10 times faster than the 1 h sample it too superimposed on the rest of the curves. Another way to show the equivalence of $\Delta \log \tau$ and $\Delta \log t$ would be to plot the yield stress, which increases with annealing time and with the strain rate, as shown in Figure 12. All curves are parallel with the same slope, n, which, incidentally, can be shown to relate to the Kohlrausch–Williams–Watts parameter by the relationship

$$n = \beta(\dot{\epsilon}\tau_{av})^{\beta} \tag{21}$$

by taking the derivative of $\log \phi(t)$ in eq 5b with respect to $\log t$.

Most creep and relaxation experiments on glassy polymers are conducted in the nonequilibrium quenched state, and therefore the result is a combination of the two opposing time-dependent behaviors; the modulus is reduced with time but with aging its rate of relaxation is slowed. Again, with the use of the simple rule, it is possible to predict the relaxation curve where the aging process is taking place simultaneously.[15]

Memory Effect

Equation 13 with the parameters as described reproduces the volumetric memory effect data quantitatively, as shown in Figure 13. However, the time for T_f to reach T_f = 30 °C at 10 °C was found to be about an order of magnitude longer than the value published by Kovacs if H_a = 56 kcal mol^{-1} was used. This meant that in this case only, the activation energy, H_a, for the Arrhenius term had

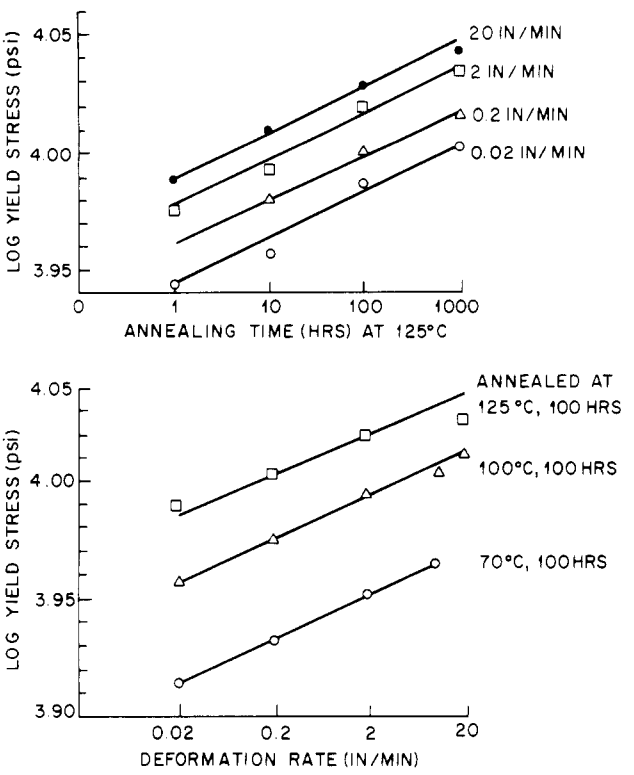

Figure 12. The yield stress vs. annealing time and vs. deformation rate are similar. Polycarbonate.

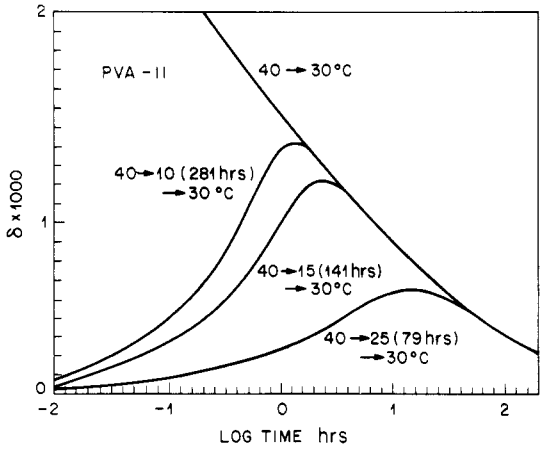

Figure 13. Memory effect, calculated for certain thermal histories that give a good representation for data by Kovacs for poly(vinyl acetate), PVA-II.[4] 40 → 10 (281 h) → 30 °C means the following: quenched from 40 to 10 °C, kept at 10 °C for 281 h, heated to 30 °C, and data taken at this instant as time zero.

to be 38 kcal mol^{-1} instead of 56 kcal mol^{-1} used elsewhere. If the temperature dependence of the distribution of relaxation times is in fact responsible for the H_a/RT term, then this Arrhenius form is also an approximation good only for a limited temperature range. The curves of δ vs. $\log t$ in Figure 13 were unaffected by the choice of values for H_a. The $\log \tau$ vs. $\log t$ plot would show the mirror image of volume data aginst the abscissa, exhibiting the minimum τ at the time where the maximum in δ appeared. The dielectric relaxation spectrum was experimentally observed to shift accordingly, as shown by the plot of the negative $\log \tau$ vs. log time in Figure 14. In Table I, the fluctuations at the end of the period following initial quench to a low temperature before backing up (Point B in Figure 3) to 30 °C were calculated and tabulated. Instead of δ, the calculated volume fluctuation was expressed in terms of the individual fictive temperatures to em-

Table I
State of Poly(vinyl acetate) Quenched from 40 °C

			conditions					
			A[a]		B[b]		C[c]	
j	$\log \tau_0(j)$	$G(j)$	$T_f(j)$	$\log \tau(j)$	$T_f(j)$	$\log \tau(j)$	$T_f(j)$	$\log \tau(j)$
1	1.5	0.04	39.9	5.28	39.8	4.82	39.6	3.92
2	1	0.16	39.6	4.78	39.5	4.32	38.7	3.42
3	0.5	0.50	38.7	4.28	38.3	3.82	36.2	2.92
4	0	1.06	36.2	3.78	35.1	3.32	30.9	2.42
5	−0.5	0.50	29.5	3.28	27.5	2.82	25.8	1.92
6	−1	0.30	17.6	2.78	17.8	2.32	25.0	1.42
7	−1.5	0.18	10.4	2.28	15.0	1.82	25.0	0.92
8	2	0.08	10.0	1.88	15.0	1.32	25.0	0.42
9	−2.5	0.08	10.0	1.28	15.0	0.82	25.0	−0.08
10	−3	0.05	10.0	0.78	15.0	0.32	25.0	−0.57
11	−3.5	0.04	10.0	0.28	15.0	−0.18	25.0	−1.08
12	−4	0.02	10.0	−0.22	15.0	−0.68	25.0	−1.58

[a] Quenched at 10 °C, and kept for 281 (160*) h. Avg T_f = 29.96 °C; avg log τ = 2.095. [b] Quenched at 15 °C and kept for 141 (140*) h. Avg T_f = 29.96 °C; avg log τ = 2.092. [c] Quenched at 25 °C and kept for 79 (90*) h. Avg T_f = 29.95 °C; avg log τ = 2.097.

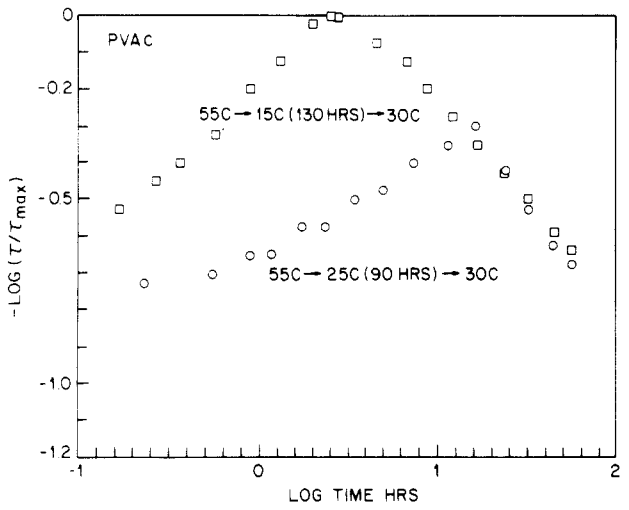

Figure 14. The dielectric relaxation time shifts to the shorter time initially and then toward the longer time as the thermal history for the memory effect in ref 4 is repeated. Poly(vinyl acetate).

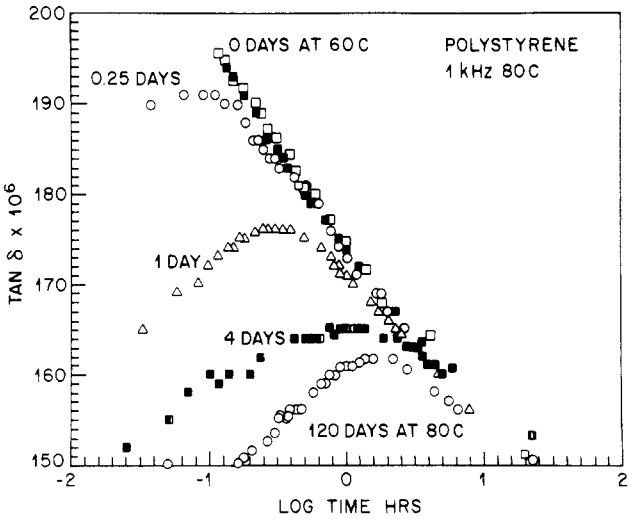

Figure 15. Dielectric tan δ vs. aging time for polystyrene repeating the memory effect history of ref 4 and 5.

phasize the physical significance for the spread. The object of the first step in quenching from 40 to 10, 15, or 25 °C was to bring the average volume to the level such that upon heating back to 30 °C it would exhibit the equilibrium volume at 30 °C. This meant that at the end of the initial quench, the average fictive temperature had to be 30 °C, which indeed is achieved. However, the distributions of fluctuations are very much at variance, as indicated by the values of $T_f(j)$, which are the measures of the individual specific volume, but which does not correlate with individual $\tau(j)$s. Thus, the domains with an unusually small density could exhibit a very long relaxation time, as noted by the related values for j = 1 or 2; in fact the largest "spike" at τ_{max} (j = 4) was less dense than the average density but at the same time exhibited a longer relaxation time than the average relaxation time, τ. The extreme cases of this type of slow fluctuations may behave as "holes" whose dynamic properties are so sluggish that they can be considered as not participating in the overall relaxation and diffusion processes,[32] and they may well contribute toward the unusual diffusion or cluster formation behavior of permeating gas and vapor molecules as suggested by Hopfenberg and co-workers.[24]

The excursion of the relaxation spectrum during the memory effect experiment first toward the short time and then back toward the long time is reflected in the appearance of the maximum in the dielectric loss tan δ with the time of aging, as shown for polystyrene in Figure 15. The sample history for these curves is duplicated from Kovacs's volumetric data and agreements on the time to reach maxima in volume and tan δ are found to be good.

Constant Rate of Heating

The differential equation, eq 3, can be made general by adding the heating rate term, $[\partial\delta/\partial T]_{T_f}\, dT/dt$.[1,4] Conditions involving the constant cooling/heating rates, rather than isothermal conditions, are particularly of interest because of the popularity of the technique with the differential scanning calorimetry. Sasabe and Moynihan[2] compared their data of this type with the dielectric relaxation time. Hodge and co-workers[8,9] have recently published several articles involving this type of analysis. Kovacs, Aklonis, Hutchison, and Ramos[4] applied their model to produce the curves for the thermal expansion coefficient vs. temperature and demonstrated that the calculated data revealed the usual features of aging/annealing found in C_p vs. T data.

Our computer program can be used for the case for the constant heating/cooling rate. The temperature dependences of the thermal expansion coefficient for the samples that were quenched from 40 to 29 °C then aged for 10^{-3}, 1, and 5 h were calculated and are shown in Figure 16. The calculated relative integrated areas and the temperatures for the peaks agree well with the differential scanning calorimetry data of Bair,[25] although the calculated

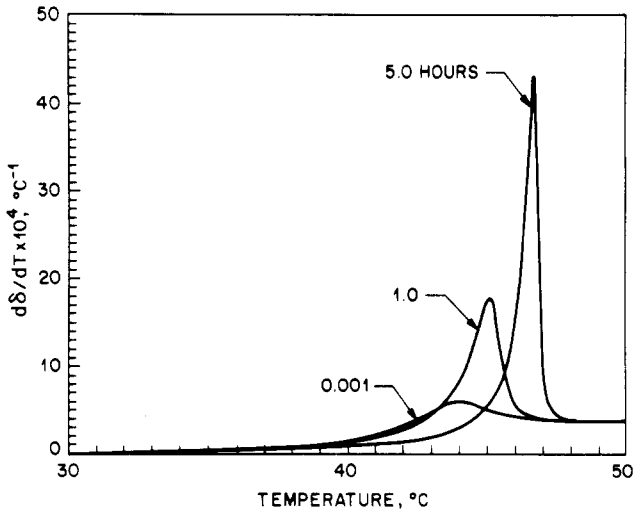

Figure 16. $d\delta/dT$ vs. T. calculated for poly(vinyl acetate), PVA-II, initially quenched from 40 to 30 °C and kept for the hours indicated, then heated at the rate of 20 °C/min.

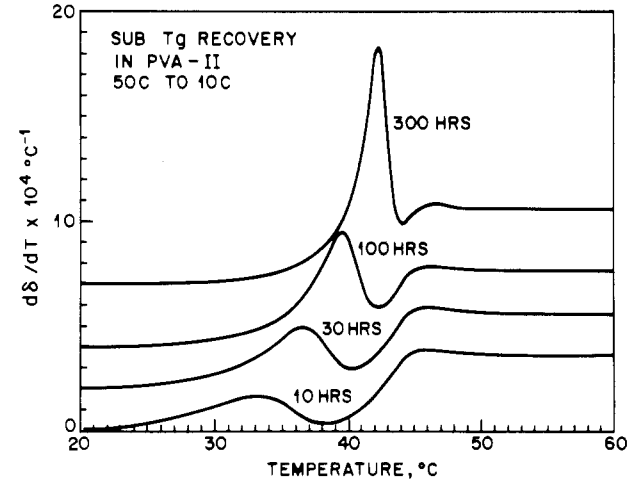

Figure 17. $d\delta/dT$ vs. T at 20 °C/min calculated for poly(vinyl acetate), PVA-II, following a severe quenching that leaves the fluctuations spread out broadly, which causes the sub-T_g peak. The hours indicate the period each sample had been kept at 10 °C before heating.

curves of Figure 16 drop much more sharply above the peak temperature than the experimental data. If the excess volume is assumed to be proportional to the excess entropy in the small temperature range near the equilibrium, then the thermal expansion coefficient should be proportional to C_p/T hence should be approximately proportional to C_p. The distribution of the density fluctuations in a quenched sample is broad. The spread of the fluctuations can cause multiple peaks depending on the combinations of the history and the heating rate.[4,8,26] Figure 17 shows the calculated results of such combinations, where the initial quenching from 50 to 10 °C was followed by 10, 30, and 100 h of waiting before the heating was begun with the rate of 20 °C/min. The sub-T_g peaks appear because of the combined effects of the slow-responding fluctuation, which tend to relax to a lower volume during the heating, and the faster responding fluctuations, which increase the volume rapidly beginning at the lower temperatures, as shown in Figure 18, where $T_f(2)$ is the fictive temperature (really the measure of the volume) of the slower responding element, $T_f(9)$ is that of the faster responding element, and T_f corresponds to the overall volume whose slope will undergo a temporary decrease, reflected in the sub-T_g peak in Figure 17. This sub-T_g peak, then, is the consequence of the behavior of the

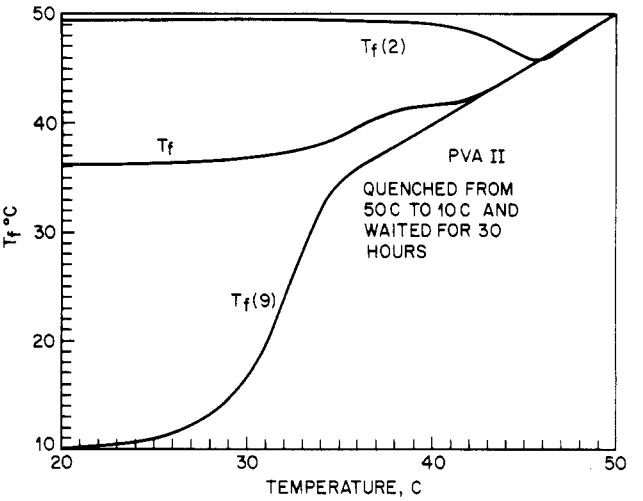

Figure 18. Reconstruction of the temperature dependence of the two extreme components and the average fictive temperature.

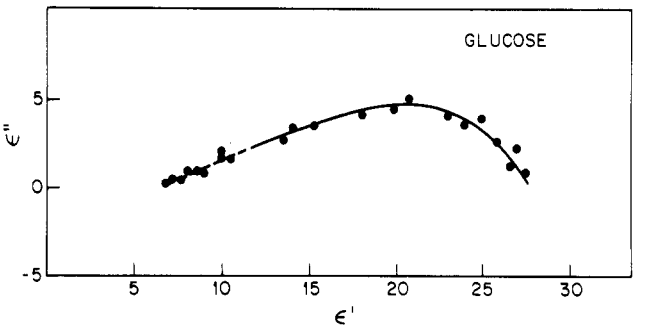

Figure 19. Cole–Cole plot for glucose.

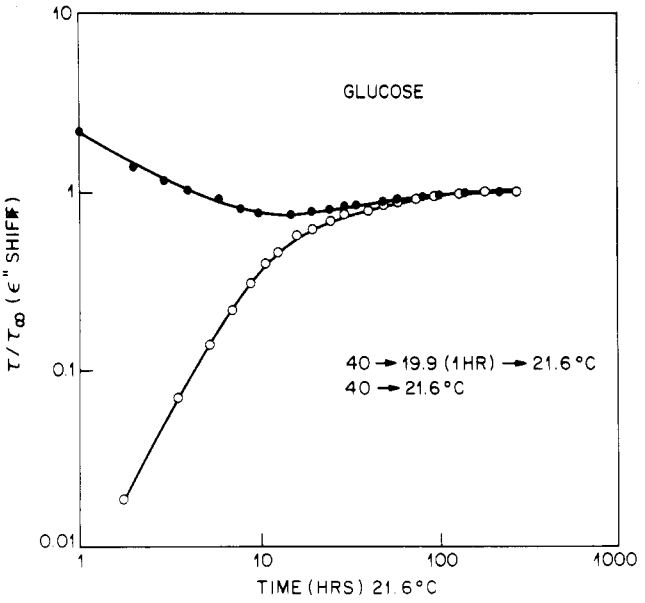

Figure 20. Shift factor during aging of glucose.

nonequilibrium density fluctuations characteristic of the behavior near T_g, and it is not necessary to invoke an additional relaxation mechanism to explain its existence.

Glucose

Kovacs[5] has shown that all of the preceding behavior is not specific to polymers but can be observed in nonpolymers such as glucose. In keeping with this contention, we obtained dielectric data on glucose that exhibited a broad distribution of relaxation times as shown in Figure 19, and the shift in the relaxation times with aging included

a slight but definite memory effect as shown in Figure 20.

Conclusion

We have analyzed aspects of the slow relaxation process associated with the glass transition. Most importantly, because the distribution of relaxation times and the aging process including the memory effect are not unique to polymers but are common to many glass-forming substances, the results obtained here will probably prove to be applicable in general. For example, from the actually measured T_g by differential scanning calorimetry at, say, 20 °C/min, (T_f for quenched glass is usually about 7 K below such T_g) the value for T_2 can be scaled accordingly, ($T_2 = T_g - 51.5$) and the entire program can be run, using $H_w = 3.70$ kcal mol^{-1}. The other adjustable parameter, H_a, can be determined form viscoelastic data or, if unknown, simply assumed to be 50 kcal mol^{-1}. Such a scheme has been applied to many different polymers with a reasonable degree of success.[15]

The general features of the process may be summarized as follows:

(1) The kinetic relaxation time for the aging follows the formula

$$\ln \tau = C + H_a/RT + H_w/R(T_f - T_2) \qquad (13)$$

(2) The dielectric and mechanical relaxation time for the loss peak at equilibrium follows the formula

$$\ln \tau = C + H_w/R(T_f - T_2)$$

where the same values for H_w and T_2 are used for the above two equations.

(3) The relaxation spectrum is assumed to remain unchanged, but the density fluctuations are found to be broadly distributed when not in equilibrium during the aging process. The extra term, H_a/RT, in eq 13 is probably due to the change in the relaxation spectrum.

(4) The *average* relaxation time for aging can be obtained from eq 13, even though no two nonequilibrium states even with identical T_f can be assumed to be the same.

(5) The sub-T_g "transition" does not necessarily mean another relaxation process but can be a consequence of the complex way the density fluctuations respond to T–t history.

Acknowledgment. Helpful discussions with G. H. Fredrickson and R. E. Robertson are gratefully acknowledged.

Nomenclature

a_i	τ_i/τ
C, $C'(T)$	adjustable parameters
C_p	specific heat at constant pressure
ΔC_p	difference in specific heat between liquidus and glass
G_i, $G(j)$	the relative strength of fluctuations, dirac δ having the relaxation time of τ_i or $\tau(j)$
H	enthalpy
H_a, H_w	apparent activation enthalpy, H_a for Arrhenius, H_w for WLF or Vogel–Fulcher expression
n	slope of log relaxation modulus vs. log time
R	universal gas constant
t	time
T	temperature
T_1	temperature below which volumetric and dielectric relaxation times diverge, it is near the usual T_g
T_2	the limiting temperature for Vogel–Fulcher expression
T_f	fictive temperature, a structural parameter corresponding to the temperature at which H, V, or S of a given glassy state intersects the equilibrium liquidus line
$T_f(j)$	a parametric expression for the volume fluctuation expressed in terms of the fictive temperature
T_g	glass transition temperature
v, v_∞	specific volume, the subscript ∞ refers to the equilibrium value
v_i, $v_{i\infty}$	the specific volume of the ith element; ∞ refers to the equilibrium
x	adjustable parameter in Narayanaswamy's formula to weigh the relative influence of temperature as x against that of the structure as $(1 - x)$ on relaxation time
α	thermal expansion coefficient
$\Delta\alpha$	difference in α for the liquidus and the glass
δ	the normalized deviation from the equilibrium value, e.g., $(v - v_\infty)/v_\infty$
δ_i, $\delta(j)$	ith (jth) component of volume fluctuations which add up to δ
ϵ	the normalized volume in excess of volume of the "T_2 glass", whose fictive temperature equals T_2, i.e., $\epsilon = \Delta\alpha(T - T_2)$
ϵ''	dielectric loss factor
τ, τ_{max}	overall relaxation time corresponding to the dielectric loss maximum
τ_0	characteristic relaxation time, which can be τ_{max}
τ_{av}	average relaxation time, e.g., $\ln \tau_{av} = \sum G_i \ln \tau_i$
τ_{eff}	reciprocal of $-\mathrm{d} \ln\delta/\mathrm{d}t$, not any relaxation time
τ_i, $\tau(j)$	relaxation time of ith (jth) dirac δ for fluctuations
ω	circular frequency in rad/s
$\phi(t)$	relaxation function of time, e.g., $\phi(t) = G_0 \exp(-(t/\tau)^\beta)$

Registry No. Poly(vinyl acetate) (homopolymer), 9003-20-7; glucose, 50-99-7.

References and Notes

(1) Moynihan, C. T.; Boesch, L. P.; LaBerge, N. L. *Phys. Chem. Glasses* **1973**, *14*, 122.
(2) Sasabe, H.; Moynihan, C. T. *J. Polym. Sci., Polym. Phys. Ed.* **1978**, *16*, 1447.
(3) Lesikar, A. V.; Moynihan, C. T. *J. Chem. Phys.* **1980**, *73*, 1932.
(4) Kovacs, A. J.; Aklonis, J. J.; Hutchinson, J. M.; Ramos, A. R. *J. Polym. Sci., Polym. Phys. Ed.* **1979**, *17*, 1097. Also: Hutchinson, J. M.; Kovacs, A. J. *Polym. Eng. Sci.* **1984**, *24* (14), 1087.
(5) Kovacs, A. J. *Fortschr. Hochpolym.-Forsch.* **1963**, *3*, 394.
(6) Williams, G.; Watts, D. C. *Trans. Faraday Soc.* **1970**, *66*, 80; *Ibid* **1971**, *67*, 1323. Williams, G. *Adv. Polym. Sci.* **1979**, *33*, 59.
(7) Chow, T. S.; Prest, W. M., Jr. *J. Appl. Phys.* **1982**, *53* (10), 6568. Chow, T. S. *Polym. Eng. Sci.* **1984**, *24* (14), 1079.
(8) Hodge, I. M.; Berens, A. R. *Macromolecules* **1981**, *14*, 1598; *Ibid* **1982**, *15*, 762.
(9) Hodge, I. M. *Macromolecules* **1983**, *16*, 898.
(10) Tool, J. *J. Am. Ceram. Soc.* **1946**, *29*, 240.
(11) Narayanaswamy, O. S. *J. Am. Ceram. Soc.* **1971**, *54*, 491. Gardon, R.; Narayanaswamy, O. S. *J. Am. Ceram. Soc.* **1970**, *53*, 380.
(12) Kovacs, A. J.; Stratton, R. A.; Ferry, J. D. *J. Phys. Chem.* **1963**, *67*, 152.
(13) Fulcher, G. A. *J. Am. Ceram. Soc.* **1925**, *8*, 339.
(14) Kovacs, A. J. *J. Polym. Eng. Sci.* **1958**, *30*, 131.
(15) Matsuoka, S. *Polym. Eng. Sci.* **1981**, *21*, 907.
(16) Brawer, S. *J. Chem. Phys.* **1984**, *81*, 954.
(17) Fredrickson, G. H.; Andersen, H. C. *Phys. Rev. Lett.* **1984**, *53*, 1244.
(18) Mashimo, S.; Nozaki, R.; Yagihara, S.; Takeishi, S. *J. Chem. Phys.* **1982**, *77* (12), 6259.
(19) Adam, G.; Gibbs, J. H. *J. Chem. Phys.* **1963**, *43*, 139. Gibbs, J. H.; DiMarzio, E. A. *J. Chem. Phys.* **1958**, *28*, 373.
(20) Robertson, R. E.; Simha, R.; Curro, J. G. *Macromolecules* **1984**, *17*, 911.
(21) Doolittle, A. K. *J. Appl. Phys.* **1951**, *22*, 1471.

(22) Cohen, M. H.; Turnbull, D. *J. Chem. Phys.* **1959**, *31*, 1164. Turnbull, D.; Cohen, M. H. *J. Chem. Phys.* **1961**, *34*, 120.
(23) Struik, L. C. E. "Physical Aging in Amorphous Polymers and Other Material" Delft, 1977, TNO Centraal Loboratorium Communication No. 565.
(24) Koros, W. J.; Chan, A. H.; Paul, D. R. *J. Membr. Sci.* **1977**, *2*, 165. Chern, R. T.; Hopfenberg, H. B.; Koros, W. J.; Sanders, E. S.; Chen, S. H. *ACS Symp. Ser.* **1983**, No. 223, 47.
(25) Bair, H. E.; Johnson, G. E.; Johnson, E. W.; Matsuoka, S. *Polym. Eng. Sci.* **1981**, *21* (14), 930.
(26) Chen, H. S.; Wang, T. T. *J. Appl. Phys.* **1981**, *52*, 5898.
(27) Johnson, G. E.; Anderson, E. W.; Matsuoka, S. *Bull. Am. Phys. Soc.* **1982**, *27* (3), 392.
(28) Leutheuser, E. *Phys. Rev. A* **1984**, *29*, 2765.
(29) Phillips, J. C. *J. Non-Cryst. Solids* **1979**, *34*, 153.
(30) Macedo, P. B.; Litovitz, T. A. *J. Chem. Phys.* **1965**, *42*, 245.
(31) Ferry, J. D. "Viscoelastic Properties of Polymers"; Wiley: New York, 1970.
(32) Monnerie, L., et al. *J. Chem. Phys.* **1984**, *81*(1), 567.
(33) Ramos, A. R.; Hutchinson, J. M.; Kovacs, A. J. *J. Polym. Sci., Polym. Phys. Ed.* **1984**, *22*, 1655.
(34) Matsuoka, S., et al. *Polym. Eng. Sci.* **1978**, *18*, (14), 1073.

Thermoelastic and Strain-Birefringence Studies on Poly(methylphenylsiloxane) Networks

Miguel A. Llorente*

Departamento de Química General y Macromoléculas, Universidad a Distancia (UNED), 28040 Madrid, Spain

Inés Fernández de Piérola

Departamento de Química Física, Facultad de Ciencias Químicas, Universidad Complutense, 28040 Madrid, Spain

Enrique Saiz

Departamento de Química Física, Universidad de Alcalá Henares, Madrid, Spain.
Received January 2, 1985

ABSTRACT: A sample of poly(methylphenylsiloxane) of known stereochemical structure was cross-linked by means of dicumyl peroxide. The resulting elastomeric networks were studied in elongation, in both the unswollen and swollen states, over the temperature range 10–70 °C. The most important experimental results obtained were values of the strain birefringence, which was found to be negative. Theoretical calculations based on rotational isomeric state theory were carried out to interpret the temperature coefficient of the unperturbed dimensions, $d \ln \langle r^2 \rangle_0 / dT$, the optical-configuration parameter, Δa, and its temperature coefficient. The agreement between theory and experiment was excellent, suggesting that intermolecular correlations, which are usually considered to be responsible for a large discrepancy between experimental and theoretical values of the stress optical properties, are very small in this polymer. Contrary to other systems, swelling the networks with decalin worsens this agreement.

Introduction

Among the configurational properties of polymeric materials, the temperature coefficient of the unperturbed dimensions, $d \ln \langle r^2 \rangle_0 / dT$, and the birefrigence, Δn, are the ones most extensively studied in elastomeric networks.[1,2] They can provide valuable information on the molecular characteristics of the chains from which the networks are constituted. The temperature coefficient of the unperturbed dimensions can be obtained from stress–temperature (thermoelastic) experiments. This technique has been proven to be very useful to obtain reliable data on many elastomeric systems.[1] The birefringence is an optical property from which one can obtain the stress–optical coefficient, C, the related optical-configuration parameter, Δa, and its temperature coefficient.

All these quantities can be evaluated theoretically from structural and configurational parameters of the polymer chains by means of the rotational isomeric state theory.[3] However, in the case of the strain-birefringence studies, poor agreement has been found between theory and experiment, particularly in the case of symmetric chains. Few studies have been performed on asymmetric chains,[4-6] in which the birefringence is usually negative, and, in this case, the agreement seems to be much better.[4,5] Another important feature of these chains is that their configurational properties usually show a strong dependence on the stereochemical structure. Therefore, it would be interesting to carry out more studies on these types of polymers, including asymmetric chains.

Poly(methylphenylsiloxane) (PMPS) is an important inorganic polymer, and the above studies would provide information about its conformation. The presence of a bulky and anisotropic side group in the chain makes the birefringence negative in the oriented polymer. Also, the special characteristics of the siloxane backbone confer very interesting properties to these chains. The inequality of the two skeletal bond angles and the long O–Si bond make the interaction between two phenyl groups, situated on the same side of the chain, attractive. This is contrary to the situation found in vinyl chains (for instance, polystyrene), in which this same interaction is repulsive.[7]

The dependence of some configurational properties of PMPS on the stereochemical structure has been studied theoretically by Mark and Ko.[8] Their calculations included the characteristic ratio and the temperature coefficient of the unperturbed dimensions. The required conformational energies were obtained from semiempirical interatomic potential energy functions and from known results on poly(dimethylsiloxane). Unfortunately, there are only a few experimental results to compare with the calculated values, and even those were obtained in polymer samples of unknown stereochemical structure.[9,10] Therefore, only a tentative comparison could be made.

The purpose of the present investigation is twofold: on the one hand, to provide more information on the configurational-dependent properties of asymmetric chains, particularly in the case of the optical properties, and on the other hand, to apply the rotational isomeric state

0024-9297/85/2218-2663$01.50/0